POLITECNICO
MILANO 1863

Department of Aerospace Science and Technology
Space Propulsion
A.Y. 2023/2024

Professor: Filippo Maggi

Monte Carlo Method for Uncertainty Quantification of SRM Burning Time

Team
GONG

Adam Lakrad	10727361	adam.lakrad@mail.polimi.it
Francesco Gardiol	10727581	francesco.gardiol@mail.polimi.it
Emanuele Gallo	10766758	emanuele.gallo@mail.polimi.it

Date: 29/05/2024

Contents

List of Figures

List of Tables

Nomenclature

BATES Ballistic Test and Evaluation System

BC   Bayern-Chemie

MB   Mass Balance

SRM   Solid Rocket Motor

TOT   Thickness Over Time

1 Introduction

This report analyzes the performance of Solid Rocket Motors (SRMs) using experimental data, emphasizing the critical need for reproducibility in performance estimates due to the inherent inflexibility of SRMs. A *Monte Carlo* simulation is used to quantify uncertainty in burning time and determine its expected average value. The case study examines the firing of nine propellant batches using a Ballistic Test and Evaluation System (BATES) motor model, specifically a Baria Motor with a center-perforated grain, as shown in Figure 1. The firing tests, from which the data is taken, were conducted at three different pressures by changing the throat area of the nozzle as exposed in Table 1, resulting in a total of 27 pressure traces. These pressure traces, obtained with a sampling frequency of 1 kHz, after a proper data analysis are illustrated in Figure 2.
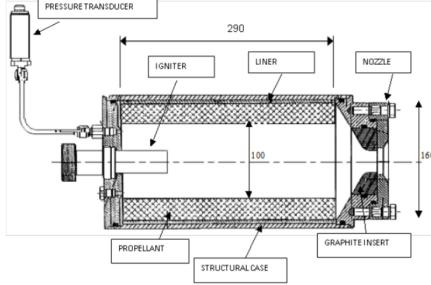

Figure 1: BATES schematics

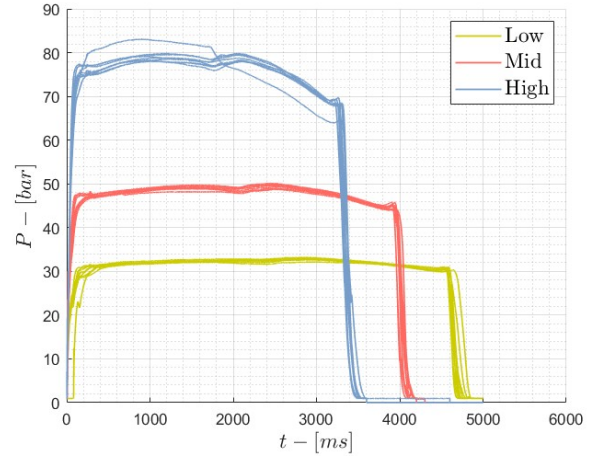| Pressure level	Throat diameter [*mm*]
High	21.81
Medium	25.25
Low	28.80

Table 1: Nozzle configurations

Figure 2: Pressure traces

By analyzing pressure traces the effect of the microscopic heterogeneity are clearly visible. First of all the typical trend due to the hump effect [4][8] can be recognized, which derives from the way the propellant is cast into the engine casing. Moreover, specific regions can be identified. The initial overshoot is caused by micro-surface irregularities triggering uneven burning. These manufacturing imperfections lead to localized high-pressure zones and a temporary increase in burn rate. As burning progresses, these irregularities diminish, stabilizing the burn rate. A mid-trace pressure decrease is primarily attributed to manufacturing reasons. Towards the trace end, a slight overshoot, known as Friedmann curl, occurs. This phenomenon is associated with the arrangement of solid particles within the grain (i.e., packing effect). These particles tend to accumulate at a specific distance from the metallic case, resulting in a localized increase in burn rate and combustion chamber pressure close to the tail-off phase [6][5]. Additionally, the propellant used is nominally identical for each batch, with its ingredients and relative abundances detailed in Table 2.

Name	Formula	Percentage [%]	Density [g/cm^3]	Δh_0 [kJ/mol]
Ammonium Perchlorate	NH_4ClO_4	68	1.95	-295.77
Aluminum	Al	18	2.7	0
HTPB	$C_{7.075}H_{10.65}O_{0.223}N_{0.063}$	14	0.92	-58

Table 2: Propellant grain formulation

2 Internal ballistics analysis

There is no theoretical model to predict the burning rate of solid propellants. Consequently, for both industrial and research purposes, various techniques have been developed to measure the ballistic properties of full-scale motors starting from small-scale ones. These techniques fall into two main categories: Thickness Over Time (TOT) and Mass Balance (MB). TOT techniques, in particular, face challenges due to non-instantaneous burnouts and are based on the conventional burning rate definition $r_b = w/t_b$, where w is the web thickness and t_b is the burning time. What sets each TOT method apart is the specific definition of burning time [2]. The present paper considers the Bayern-Chemie technique.

2.1 The Bayern Chemie method

The challenge lies in identifying the correct burning time, due to the ignition transient. The Bayern-Chemie (BC) method addresses this by identifying two main time intervals: action and burning time. The action interval is determined by identifying the instants t_A and t_G where the pressure crosses 5% of its maximum value. Furthermore, during ignition, oscillatory behavior may cause the pressure trace to cross this threshold multiple times. In such cases, the last upward pressure change before steady-state is chosen. If the ignition transient includes a pressure peak comparable to the maximum pressure, this peak is discarded. Once the action time is determined the reference pressure (p_{ref}) is computed as defined in Equation 1. From this, by examining the pressure traces, the burning time can be inferred as $t_b = t_E - t_B$ by identifying the points t_B and t_E, where the pressure trace crosses the value p_{ref}. The relative effective pressure is then computed as shown in Equation 1:

$$p_{ref} = \frac{1}{2(t_G - t_A)} \int_{t_A}^{t_G} p \, dt \qquad p_{eff} = \frac{\int_{t_B}^{t_E} p \, dt}{t_{burn}} \tag{1}$$

1

The burning rate r_b is retrieved by inserting the found t_b value in its definition. With these concepts at hand, it becomes feasible to determine the mean values and standard deviations of the coefficients a and n, pre-exponential factor and exponential factor respectively. This is done by performing a fitting on the 27 pairs of the previously determined effective pressures and the relative burning rate according to Vielle's law (Equation 2).

Figure 3 shows that the found values follow an exponential trend depending on pressure. This is coherent with the Vielle's law:

$$r_b = a \cdot P^n \tag{2}$$

The mean values and standard deviations of the declared parameters resulting from this analysis are summarized in the following Table 3:

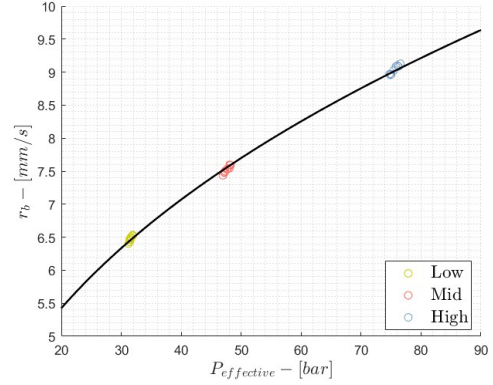| Parameter	Value	
$a\left[\frac{m/s}{bar^n}\right]$	Mean value	$1.7279 \cdot 10^{-3}$
	Standard deviation	$1.8404 \cdot 10^{-5}$
$n[-]$	Mean value	0.3820
	Standard deviation	$2.7353 \cdot 10^{-3}$

Table 3: Vielle's law fitting results

Figure 3: Vielle's law fitting

2.2 Baria combustion

For each of the 27 motor pressure traces the experimental value of c^* is computed as:

$$c^* = \frac{\int_{t_A}^{t_G} P(t)dt}{M_P} A_t \tag{3}$$

The results are shown in Figure 4, which highlights the distinction between high, medium, and low pressure tests. From these values, the characteristic velocity mean value $\bar{c}^*$ is computed to be $1522.54\,\mathbf{m/s}$, with a standard deviation σ_{c^*} of $8.95\,\mathbf{m/s}$. With this information and from the knowledge of the coefficients of Vielle's law, the motor behaviour under steady-state conditions can be simulated using the formula:

$$P(t) = \left(\bar{c}^* a \rho \frac{A_b(t)}{A_t} \right)^{\frac{1}{1-n}} \tag{4}$$

Due to the short burning time, the throat area can be assumed constant, and pressure variations can be attributed solely to changes in the burning area over time. For each time instant the burning area is computed as $A_b(t,p) = A_{internal}(t,p) + 2A_{side}(t,p)$. Where $A_{internal}(t,p)$ is the core radial burning surface, while $A_{side}(t,p)$ is the surface of the circular crown for transversal burning. Then, $P(t_k)$ is computed from Equation 4 and $r_b(t_k)$ from Vielle's law. At the end, the quantities useful to restart the cycle are updated. In conclusion, the modelled steady-state pressure profile and its corresponding burning time are derived. Using the model, plots illustrating the burning times and pressure profiles are depicted in Figure 5. As seen, the model cannot simulate the real transient behaviours and the combustion is stopped when one of the burning surfaces becomes zero. Naturally, the model does not show the typical trends associated with manufacturing imperfections.
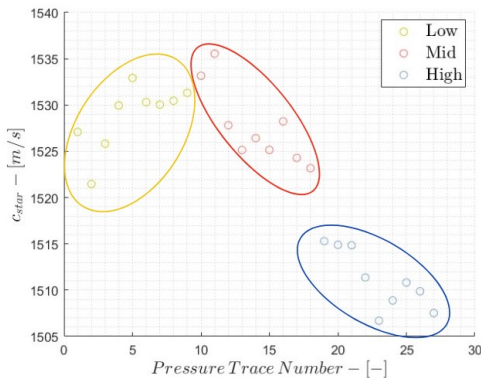

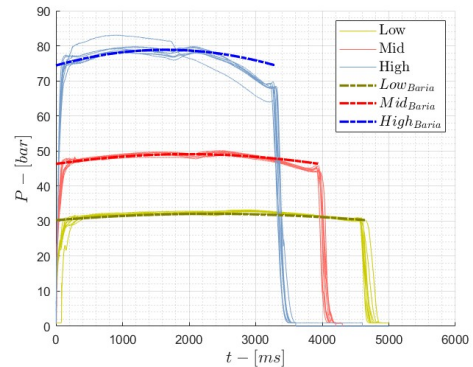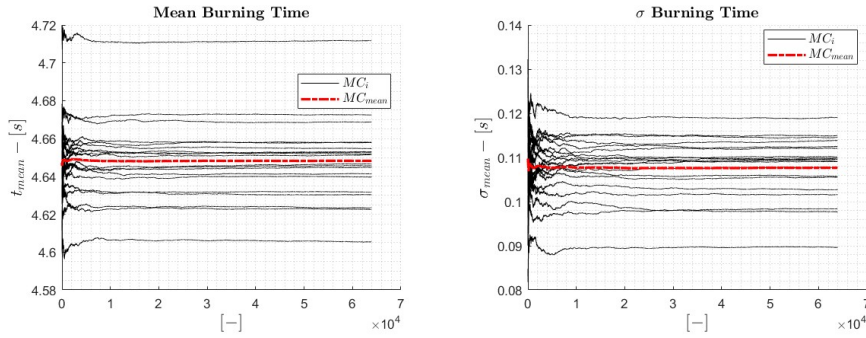Figure 4: c^* for each pressure trace

Figure 5: Comparison of Baria combustion simulation with the experimental pressure traces

3 Monte Carlo simulation

Based on the data provided in Table 3 and on the values of $\bar{c}^*$ and σ_{c^*}, a *Monte Carlo* simulation is proposed to ascertain the burning time for each pressure level, in order to determine how the intrinsic variability affects the internal ballistics. This simulation, based on the rationale proposed in [1], necessitates the understanding of the distribution type of input parameters. Given the standard deviation and mean value variability of parameters a, n, c^*, a normal distribution is deemed

suitable, implying a natural variability of the process. Thus, a population of size N is randomly shaped on Gaussian distribution for a, n and c^*. All possible combinations are randomly outlined, yielding N^3 triplets. This procedure allows not only to include process uncertainties, typical of real tests, but also to better monitor the convergence of the simulation, avoiding the presence of steps due to a sudden change of the input variables. Each triplet is subsequently fed into the Baria code, described previously in subsection 2.2, to compute the corresponding pressure traces and relative burning time. A vector is incrementally constructed to aggregate all generated burning times. Throughout this process, a cumulative mean and standard deviation of computed burning times are determined to track convergence. For each nozzle throat diameter, a multiple *Monte Carlo* simulation is performed, using a parallel computation to enhance the calculation processes. This procedure enables the analysis of multiple pressure traces, comparing the single trends and allowing to better determine the mean burning time. Convergence evaluation involves extracting the last fifth of the N^3 elements from vectors representing the mean of burning times. The mean of these extracted values is then determined. Convergence is considered attained if the relative residual between each extracted value and the precedent falls below a predefined threshold, typically set at 0.01%. In addition, the convergence can be also evaluated directly through the analysis of the mean of burning times trend. In the specific scenario under examination, a population consisting of 40 samples for both a, n and c^* is determined to be adequate for achieving convergence with the desired precision. In Figure 6, the mean burning time and standard deviation for the low pressure nozzle configuration is reported, whereas the other two configuration results are in the Appendix 4.1. The *Monte Carlo* simulation reveals that both mean and the standard deviation converge, but the latter has a slower pace compared to the mean burning time. The *Monte Carlo* simulation is performed for each nozzle 20 times. The maximum relative residual for t_b is on the order of 10^{-4} %, confirming the convergence of the simulation. This shows that the chosen population of 40 samples is sufficient to converge with an adequate precision; otherwise, it would have been necessary to increase the sample size. For each nozzle configuration, the selected final burning time $\bar{t}_b$ is the final value of the average of all the *Monte Carlo* simulation mean burning times, and similarly, the standard deviation mean value $\bar{\sigma}_{t_b}$ has been computed using the same method. Furthermore, a high density of plots is present around the mean value, whereas two offset trends are present. All the *Monte Carlo* simulation mean burning times fall within the range defined by the $\bar{t}_b$ and $\bar{\sigma}_{t_b}$.

Figure 6: Low pressure *Monte Carlo* simulation trends

The simulation outcomes for each pressure level are reported in Table 4. As expected from the experimental traces in Figure 2, the mean burning time is higher for the lower pressure trace and lower for the higher pressure trace.

Parameter	Pressure range		
	Low	**Medium**	**High**
$\bar{t}_b$ [s]	4.6482	3.9578	3.2973
$\bar{\sigma}_{t_b}$ [s]	0.1077	0.0980	0.0858

Table 4: *Monte Carlo* simulation results in the three pressure ranges

4 Conclusion

From Table 5, the relative uncertainty of a, n and $\bar{c}^*$ is amplified during the computation of t_b . The discrepancy between the three burning time uncertainties is caused mainly by the different t_b for the different nozzle configurations.

Pressure level	Relative uncertainty on $\bar{t}_b$	Relative uncertainty on a	Relative uncertainty on n	Relative uncertainty on $\bar{c}^*$
Low	2.32%			
Medium	2.48%	1.07%	0.72%	0.59%
High	2.60%			

Table 5: Relative uncertainties comparison

The low values of relative uncertainties, defined as the ratio between the standard deviation and the mean value for the same quantity, clearly highlight that the numerical model utilized in this work accurately approximates the Baria motor. This approach could be used not only to analyze existing engines but also to assist in the design of future ones. Furthermore, the use of the *Monte Carlo* method allows to compute the burning time and its relative uncertainty based on a limited number of firing tests, thus reducing the overall cost.

References

[1] HW Coleman and WG Steele Jr. "Uncertainty in a result determined from multiple variables". In: *Experimentation, Validation, and Uncertainty Analysis for Engineers* 3 (2009), pp. 61–83.

[2] R. Fry, L. DeLuca, G. Gadio, R. Fredericks, R. Strecker, H.-l. Besser, A. Whitehouse, J.-c. Traineau, D. Ribereau, and J. Reynaud. "Solid propellant burning rate measurement methods used within the NATO propulsion community". In: *37th Joint Propulsion Conference and Exhibit* (July 2001). DOI: 10.2514/6.2001-3948. URL: https://doi.org/10.2514/6.2001-3948.

[3] Ronald W. Humble, Gary N. Henry, and Wiley J. Larson. *Space Propulsion Analysis And Design*. The McGraw-Hill Companies, Inc., 1995.

[4] T. Kallmeyer and L. Sayer. "Differences between actual and predicted pressure-time histories of solid rocket motors". In: *18th Joint Propulsion Conference* (June 1982). DOI: 10.2514/6.1982-1094. URL: https://doi.org/10.2514/6.1982-1094.

[5] A. Messner. "Transient coning in end-burning solid propellant grains". In: *16th Joint Propulsion Conference* (June 1980). DOI: 10.2514/6.1980-1138. URL: https://doi.org/10.2514/6.1980-1138.

[6] Stefano Mini, Fabrizio Ponti, Alessandro Brusa, Roberto Bertacin, and Barbara Betti. "Prediction of Tail-Off pressure peak anomaly on Small-Scale rocket motors". In: *Aerospace* 10.2 (Feb. 2023), p. 169. DOI: 10.3390/aerospace10020169. URL: https://doi.org/10.3390/aerospace10020169.

[7] George P. Sutton and Oscar Biblarz. *Rocket Propulsion Elements*. John Wiley and Sons, Inc., Hoboken, New Jersey, 2017.

[8] J. Terzic, B. Zecevic, M. Baskarad, A. Catovic, and S. Serdarevic-Kadic. "Prediction of internal ballistic parameters of solid propellant rocket motors". In: *Problemy Mechatroniki : uzbrojenie, lotnictwo, inżynieria bezpieczeństwa* (Jan. 2011), pp. 7–26. URL: http://yadda.icm.edu.pl/yadda/element/bwmeta1.element.baztech-article-BWA0-0050-0009/c/httpwww_bg_utp_edu_plartpm20nr20420117-2620nr2041p20terzic20zecevic.pdf.

Appendix

4.1 Medium and High pressure Monte Carlo simulation results
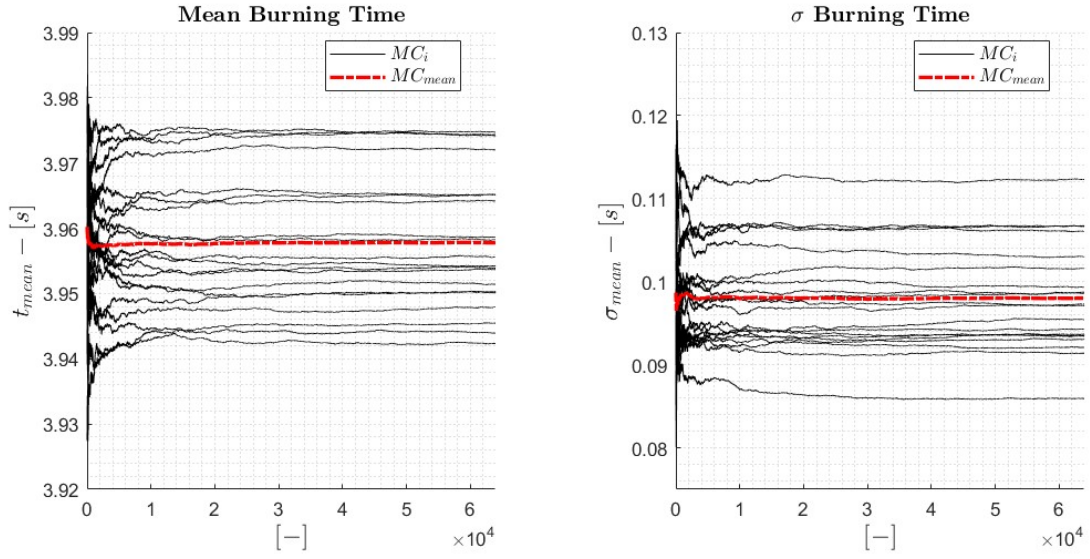

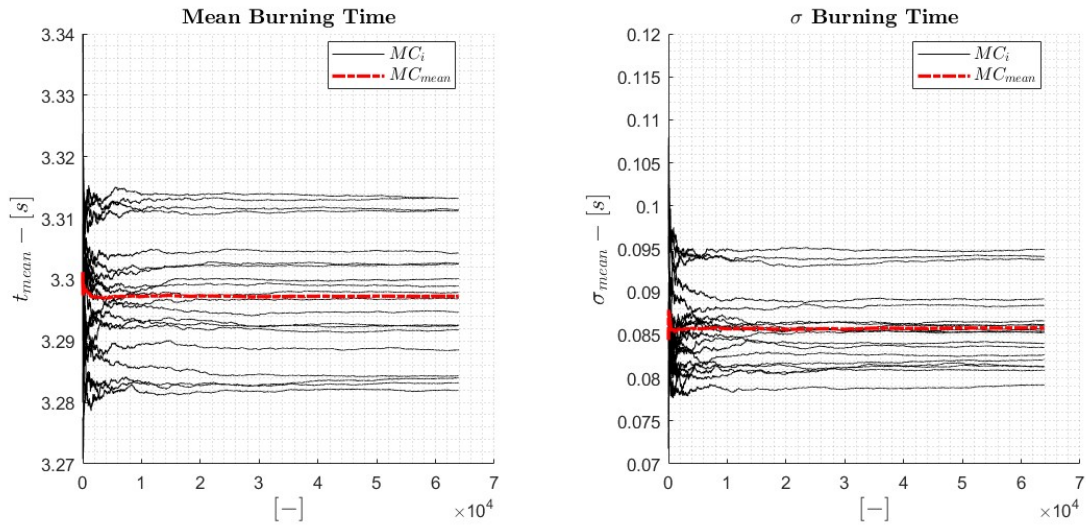Figure 7: Medium pressure Monte Carlo simulation mean t_b trend

Figure 8: High pressure Monte Carlo simulation mean t_b trend